RAPID COMMUNICATIONS

PHYSICAL REVIEW B VOLUME 43, NUMBER 11 15 APRIL 1991-I

Magnetotunneling in a coupled two-dimensional–one-dimensional electron system

Seigo Tarucha and Yoshiro Hirayama
NTT Basic Research Laboratories, Musashino-shi, Tokyo 180, Japan
(Received 11 December 1990)

Magnetotunneling in a double-barrier diode with a restricted lateral dimension was studied. The zero-field tunneling current shows fine structures supposed to be due to mixing of two-dimensional emitter subbands with one-dimensional subbands in the double-barrier region. Application of a magnetic field causes a depopulation of the current structure. This arises from couplings of electromagnetic subbands with and without conservation of the quantum numbers.

Resonant tunneling through zero- and one-dimensional (0D and 1D) systems was recently observed using double-barrier (DB) diodes with two dimensionally and one dimensionally restricted lateral dimensions, which we call 0D and 1D resonant-tunneling diodes (RTDs). Reed *et al.*[1] used reactive-ion-beam etching to fabricate a 0D RTD with an $Al_xGa_{1-x}As/In_yGa_{1-y}As$ DB structure, and more recently we used focused Ga ion-beam (Ga-FIB) implantation to fabricate 1D and 0D RTDs with an $Al_xGa_{1-x}As/GaAs$ DB structure.[2] The current-versus-voltage (I-V) characteristics of these RTDs exhibited a series of peaks due to resonant tunneling associated with the laterally confined 0D and 1D subbands. However, the assignment is not explicitly given when we consider the effect of lateral confinement in the emitter because this effect makes resonant tunneling feasible from 1D to 0D systems in a 0D RTD and from 2D to 1D systems in a 1D RTD as theoretically predicted in the first case by Bryant.[3] When the lateral confinement is different between the emitter and DB-well regions, subband mixing causes an electron to tunnel from a laterally confined emitter subband below the Fermi level to a number of laterally confined DB-well subbands. This process generates well-defined current peaks corresponding to the laterally confined subband structure in the DB well when the lateral confinement is much weaker in the emitter than in the DB well.[1,2] However, no evident observation to define the subband mixing effect has so far been reported.

This Rapid Communication presents a magnetic-field study on the subband mixing effect observed in a 1D RTD. A magnetic field has been used as a powerful tool to investigate tunneling characteristics of conventional DB diodes.[4,5] The magnetic quantization theory predicts a transition from laterally confined electric subbands to electromagnetic subbands in the 1D RTD when a magnetic field is applied parallel to the tunneling direction. The hybrid subbands in the emitter shift to high energies with magnetic field more largely than those in the DB well because of the weaker electrostatic confinement. This difference allows spectroscopic investigation of the subband mixing effects.

Our sample had a DB structure of a 6-nm-GaAs well and two 7-nm-$Al_{0.5}Ga_{0.5}As$ barriers, sandwiched between two 4-nm-undoped GaAs spacers. The GaAs contact regions (emitter and collector) were doped with Si to 1×10^{18} cm^{-3}. The heterojunctions confined the electron system in the **z** direction. Lateral confinement in the **x** direction was imposed by Ga-FIB implantation in the epitaxial surface, leaving a single rectangular space of $(L_x \times L_y)$ ($L_x = 155$ nm and $L_y = 400$ nm). The confining potential was formed by the implantation-induced depletion and approximated by a parabolic profile with a flat region in the center. The depletion depth of 70 ± 5 nm was evaluated in the DB well from measurements of resonant current peaks,[2] while that of 30 ± 5 nm in the contact was evaluated from the doping level.[6] The L_y value was large enough to assume the free-electron motion in the **y** direction at the measurement temperature of 1.5 K. The details of the sample fabrication were described previously.[2] Large area diodes with diameter ≥ 2 μm exhibited a tunneling current peak at 0.3 ± 0.05 V with 12 ± 2 A/cm^2. The peak voltage is larger than the value $(2\varepsilon_0/e)$ given by the calculated ground-state subband energy ε_0 of 71 meV. This is mostly due to the band bending as discussed in several previous papers.[5,7] The observed peak voltage shifted higher in voltage up to 0.5 ± 0.05 V with decreasing L_x. This voltage shift is probably due to the up shift of the conduction band in the DB region relative to that in the contact that results from the DB region being laterally restricted by the implantation.[2] The same effect was previously demonstrated for a 0D RTD using a three-dimensional self-consistent band diagram calculation.[8]

Figure 1 shows the I-V characteristic in the absence of a magnetic field. The I-V curve exhibits a series of major current peaks, which are numbered as $n=0,1,\ldots$ beginning from the lowest in voltage. These kinds of current peaks were previously observed in a similar diode structure, and assigned, according to the calculation of resonance positions, to resonant tunneling associated with respective 1D subbands in the DB well.[2] With the same calculation, the major current peaks can be assigned to resonant tunneling associated with the 1D subbands in the DB well. For this assignment we have calculated a one-dimensional self-consistent band diagram to correct the band bending in the **z** direction,[9] and assumed that an electron is injected into the DB well without relaxing in the accumulation layer adjacent to the barrier because of the small accumulation layer width of approximately 4 nm calculated for our diode. We have also assumed that the band bending caused by the lateral restriction simply

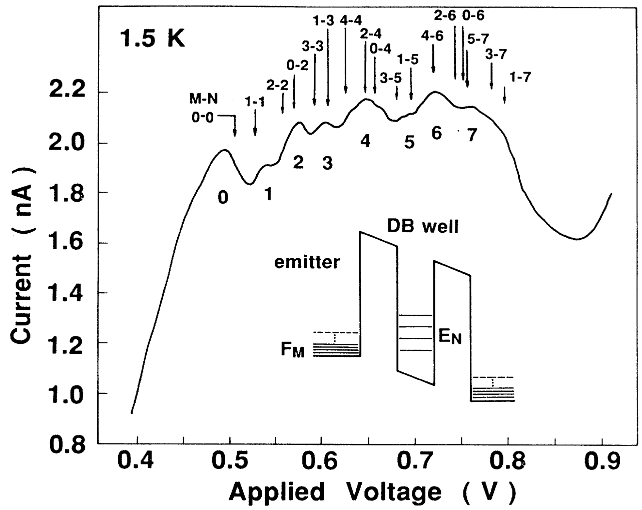

FIG. 1. I-V characteristics of a 1D RTD. The arrow defined by M-N indicates the calculated peak associated with the Mth emitter subband and the Nth DB-well subband. The whole set of arrows are shifted by about 0.25 V.

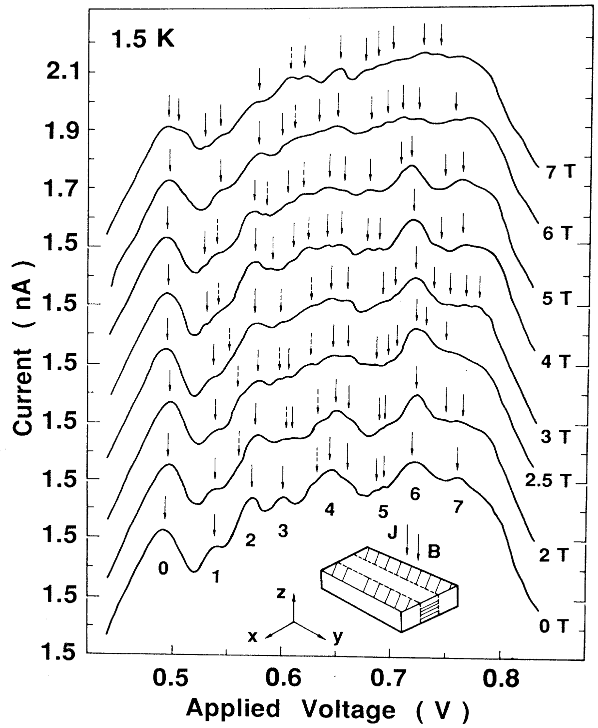

FIG. 2. I-V characteristics under a parallel magnetic field. The arrows indicate the observed current peaks and shoulders.

gives a voltage offset to the observed peak position.[2] The importance of the present result is the observation of fine structures around the $n=4$ and 5 peaks. These structures were not resolved in our previous work probably due to the higher measurement temperature of 4 K. They suggest coupling of various 2D subbands in the emitter to the respective 1D subbands in the DB well. These fine structures are rather faint probably due to the impurity scattering effect in the contact.

To investigate the subband mixing effect we have calculated a sequential tunneling current from the 2D subbands in the emitter to the 1D subbands in the DB well. Here, electrons tunnel elastically into the DB well, conserving parity in the **x** direction, momentum in the **y** direction, and total energy. Tunneling current $J_{M\text{-}N}$ from the Mth ($M=0,1,2,\ldots$) emitter subband with energy F_M to the Nth ($N=0,1,2,\ldots$) DB-well subband with energy E_N starts to flow when $E_N=\varepsilon_F$, Fermi energy, and it is maximum when $E_N=F_M$. This model leads to a current peak voltage so as to compensate for the energy difference of E_N and F_M. The calculated peak positions are shown by the arrows with M-N in Fig. 1. The relative positions are compared with the measured current peaks by shifting the whole set of the calculated peak positions by about 0.25 V. The reason for this peak shift was described before. The peak spacings are corrected using a self-consistent band diagram calculation.[9] Here, we consider $J_{M\text{-}N}$ with $N \geq M$ because the subband coupling intensity becomes significantly small when $N<M$. The calculated peak positions seem to explain the measured current spectrum reasonably well, although the $n=1$ and 2 peaks are not well resolved. The depletion depths of 30 and 67 nm are assumed for the emitter and DB well, respectively, to reproduce the observed current structure.[10] These values agree well with the previous estimates.

Figure 2 shows the I-V characteristic in the presence of a parallel magnetic field B. The structures indicated by the arrows are more clearly identified when we take the derivatives (dI/dB). Several changes in the I-V curves are apparent for $B>2$ T: a weak shoulder appears in the low voltage of the $n=2$ peak and shifts to low voltage as shown by the dashed arrows. A similar low voltage shift is observed for the weak structures in the low voltages of the $n=3$ and 4 peaks as also shown by the dashed arrows. In addition, several new, weak peaks and shoulders appear for $B \geq 3$ T, but their magnetic field dependences are not uniform. In contrast the main peaks of $n=0$ and 2 shift only slightly with increasing field. The whole current spectrum becomes ambiguous with B due to these nonuniform shifts of peaks and shoulders as well as to the broadening of peaks and shoulders. The spectral broadening suggests that the subband mixing is disturbed by the formation of hybrid electromagnetic subbands. The voltages of peaks and shoulders in the I-V curves are plotted versus B in Fig. 3. The filled, half-filled, and open circles represent the large, medium, and small features, respectively. The crosses represent the same plots for a large area ($>2\times2$ μm^2) sample. The solid lines connect the changes of the related peaks and shoulders. Figure 3 clearly shows the low-voltage shifts of the lower branches originating from the $n=2$, 3, and 4 peaks. In contrast, the shift to high voltage of the upper branch originating from the $n=6$ peak seems to be closely related to the magnetic field. The other peaks and shoulders exhibit more gradual magnetic field dependences. On the other hand, the large area sample exhibits a single, large current peak whose position is almost unchanged with B.

Application of parallel magnetic field to a large area

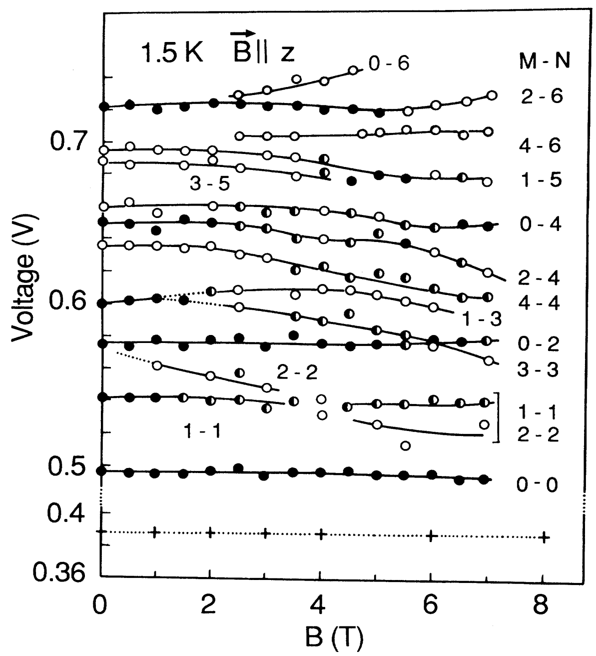

FIG. 3. Voltage positions of current peaks and shoulders as a function of magnetic field. The lines connect the changes of the related peaks and shoulders.

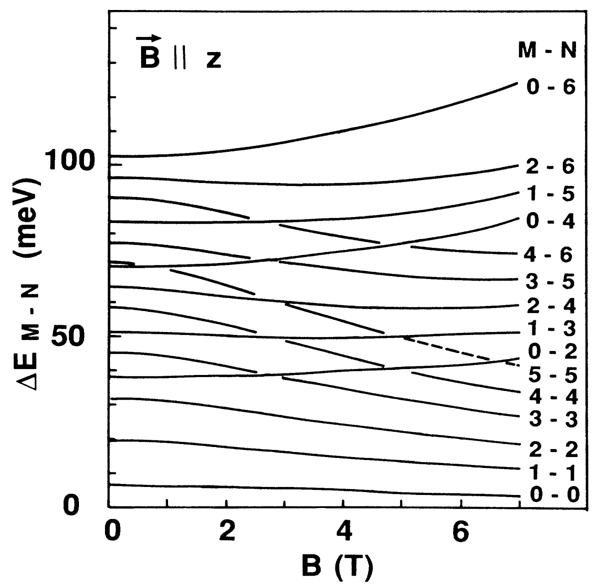

FIG. 4. Calculated energy difference between the Mth electromagnetic emitter subband and the Nth electromagnetic DB-well subband. The broken line represents $\Delta E_{5\text{-}5}(B)$ for the emitter subband above the Fermi level.

DB structure quantizes the 3D electron system in the emitter and the 2D electron system in the DB well into equivalent Landau levels. A tunneling current peak appears when the Landau level in the DB well reaches the Landau level of the same quantum number in the emitter, as the applied voltage is increased. This tunneling process was previously reported,[11] and we assume it is also responsible for the current peak observed in our large area diode. The Landau quantization in a DB structure with a restricted lateral dimension is not equivalent between the emitter and DB well because of the difference in electrostatic lateral confinement. When the electrostatic potential is modeled by a harmonic approximation given by $\frac{1}{2}m^*\omega_{w0}^2x^2$ in the DB well and $\frac{1}{2}m^*\omega_{e0}^2x^2$ in the emitter, the confined eigenenergies are given by

$$E_N=\varepsilon_0+(N+\tfrac{1}{2})\hbar\omega_w \quad (N=0,1,2,\ldots) \text{ (well)} \qquad (1)$$

and

$$F_M=\frac{\hbar^2}{2m^*}k_z{}^2+(M+\tfrac{1}{2})\hbar\omega_e \quad (M=0,1,2,\ldots) \text{ (emitter)}, \qquad (2)$$

where $\omega_w=(\omega_{w0}^2+\omega_c^2)^{1/2}$ and $\omega_e=(\omega_{e0}^2+\omega_c^2)^{1/2}$, where ω_c is the cyclotron frequency. E_N (F_M) increases with B, and the field dependence is larger for the larger N (M), and also for the weaker electrostatic confinement. When $h\omega_c$ is smaller than either $\hbar\omega_{w0}$ or $\hbar\omega_{e0}$, the tunneling current is significantly produced by mixing the emitter subbands with the DB-well subbands with the requirement of $M\text{-}N=2l$ (l: integer). This current provides a peak whose voltage position shifts with B by $\Delta V(B)=2[E_{M\text{-}N}(B)-E_{M\text{-}N}(0)]/e$, where $E_{M\text{-}N}(B)=E_N(B)-F_M(B)$.

Figure 4 shows the calculated $\Delta E_{M\text{-}N}(B)[=E_{M\text{-}N}(B)-E_{M\text{-}N}(0)]$. Values of 3 meV for $\hbar\omega_{e0}$ and 16 meV for $\hbar\omega_{w0}$ are assumed for reproducing the fine structures observed in the $n=4$ and 5 peaks at $B=0$. $\hbar\omega_c\leq 12$ meV $<\hbar\omega_{w0}$ for $B\leq 7$ T. Here, we consider tunneling between the hybrid subbands with $N\geq M$ as described before. When we consider the band bending effect, a magnetic-field induced shift of measured current structure is expected to be given by $2\Delta E_{M\text{-}N}(B)/ef$, where f is the correction factor of about 0.7.[9] The field dependences of $\Delta E_{M\text{-}N}$ become complicated due to the large difference between ω_{e0} and ω_{w0}. Particularly, $\Delta E_{M\text{-}N}$ with $N=M$ or conservation of the quantum number decreases as B is increased. This $\Delta E_{M\text{-}N}$ decrease becomes more obvious for the larger $N(=M)$. The present calculation neglects several important effects such as non-parabolicity of electrostatic potential and Landau level broadening. Nevertheless, we find a qualitative agreement of the calculated $\Delta E_{M\text{-}N}(B)$ with the magnetic-field induced shifts of peaks and shoulders shown in Fig. 3. The calculated $\Delta E_{2\text{-}2}$ and $\Delta E_{0\text{-}2}$ are close to each other at $B=0$ T, and, due to the pronounced downward shift of $\Delta E_{2\text{-}2}$, gradually separate with increasing B. The same field dependence is seen for $\Delta E_{3\text{-}3}$ and $\Delta E_{1\text{-}3}$, and for $\Delta E_{4\text{-}4}$ and $\Delta E_{0\text{-}4}$ ($\Delta E_{2\text{-}4}$). This behavior compares well with the observed field dependences of $n=2$, 3, and 4 peaks. The structures assigned to $\Delta E_{2\text{-}2}$, $\Delta E_{3\text{-}3}$, and $\Delta E_{4\text{-}4}$ are fairly weak. The large hybrid subband level broadening may be the reason. No current structures corresponding to $\Delta E_{M\text{-}N}$ with $N=M\geq 5$ are observed probably because the emitter subbands with $M\geq 5$ are above ε_F as shown by the broken line in Fig. 4. The field dependences observed for the other current peaks and shoulders are also explained when assigned to the subband couplings as indicated by M-N in Fig. 3.

In summary, we used magnetic-field effects to study tunneling characteristics of a 1D RTD. The zero-field I-V characteristic exhibited fine structures supposed to be due to mixing of 2D emitter subbands with 1D DB-well subbands. Application of a magnetic field gave rise to a pronounced depopulation of the structures on the tunneling current spectrum. This was explained in terms of tunnelings with and without conservation of the quantum numbers.

The authors are grateful to Tadashi Saku for the sample preparation, Yasuhiro Tokura for a self-consistent band diagram calculation, and to Tsuneya Ando and Yoshiji Horikoshi for valuable discussions on the tunneling process. The authors also wish to thank Tatsuya Kimura for his advice throughout this work.

[1]M. A. Reed, J. N. Randall, R. J. Aggarwal, R. J. Matyi, T. M. Moore, and A. E. Wetsel, Phys. Rev. Lett. **60**, 535 (1988).

[2]S. Tarucha, Y. Hirayama, T. Saku, and T. Kimura, Phys. Rev. B **41**, 5459 (1990).

[3]G. W. Bryant, Phys. Rev. B **39**, 3145 (1989).

[4]E. E. Mendez, L. Esaki, and W. I. Wang, Phys. Rev. B **33**, 2893 (1986).

[5]V. J. Goldman, D. C. Tsui, and J. E. Cunningham, Phys. Rev. B **35**, 9387 (1987).

[6]S. Nakata, Y. Hirayama, S. Tarucha, and Y. Horikoshi (unpublished).

[7]M. A. Reed, W. R. Frensley, W. M. Ducan, R. J. Matyi, A. C. Seabaugh, and H.-L. Tsai, Appl. Phys. Lett. **54**, 1256 (1989).

[8]M. A. Reed, J. N. Randall, J. H. Luscombe, W. R. Frensley, R. J. Aggarwal, R. J. Matyi, T. M. Moore, and A. E. Wetse, Festkoerperprobleme **29**, 267 (1989).

[9]We have calculated the band diagram without lateral restriction in the same way as reported by Reed *et al.* (Ref. 7) and found that $35 \pm 3\%$ of the voltage increment applied in the resonance region is used to compensate for the energy separation between the emitter and DB-well subbands.

[10]The calculated energies imposed by the lateral confinement are 0.4, 1.9, 4.2, 7.4, 11.6, and 16.6 meV, respectively, for the lowest to the 5 excited 1D subbands in the DB well, and 3.3, 12.6, 26.2, 41.8, 58.2, and 75.2 meV, respectively, for the lowest to the 5th excited 2D subbands in the contacts. Here, the lateral potential barrier height is assumed to be 1.5 eV for an electron in the n-type emitter (Ref. 2), while it is assumed to be 1.2 eV for an electron in the DB well by taking into account the band bending and the 2D subband energy.

[11]M. L. Leadbeater, A. Celeste, J. C. Portal, G. Hill, and A. Pate, Phys. Rev. B **39**, 3438 (1989).